INSTITUTE OF PHYSICS PUBLISHING JOURNAL OF PHYSICS: CONDENSED MATTER

J. Phys.: Condens. Matter **15** (2003) 7891–7899 PII: S0953-8984(03)65554-2

Search for new half-metallic ferromagnets in semi-Heusler alloys NiCrM (M = P, As, Sb, S, Se and Te)

Ming Zhang, Xuefang Dai, Haining Hu, Guodong Liu, Yuting Cui, Zhuhong Liu, Jinglan Chen, Jianli Wang and Guangheng Wu

State Key Laboratory for Magnetism, Institute of Physics, Chinese Academy of Sciences, Beijing 100080, People's Republic of China

E-mail: zm_info@yahoo.com.cn (Ming Zhang)

Received 2 July 2003
Published 7 November 2003
Online at stacks.iop.org/JPhysCM/15/7891

Abstract

The first-principles calculation within density-functional theory is used to search for new candidates of half-metallic ferromagnets in semi-Heusler alloys NiCrM (M = P, As, Sb, S, Se and Te). Our calculations predict that NiCrP, NiCrSe and NiCrTe are half-metallic ferromagnets (HMFs) with magnetic moments of nearly 3 or 4 μ_B/fu and HM gaps of 0.263, 0.047 and 0.102 eV, respectively. Other compounds are so-called nearly HMFs. Substitution of the sp atoms cannot be responsible for the formation of the band gap, but results in a shift in the Fermi level and the loss of half-metallicity. The half-metallicity of NiCrP and NiCrTe can be retained when the lattice parameter is changed by about 2%–3%.

1. Introduction

The rapidly developing field of spintronics [1, 2] holds much promise for the future. Widely possible applications are in non-volatile magnetic random access memories (MRAMs), but also an increase in the efficiency of optoelectronic devices and even a self-assembled quantum computer are envisaged [3]. The key ingredient is the source of the spin-polarized charge carriers. An ideal choice is the half-metallic ferromagnets (HMFs), i.e. the minority band is semiconducting with a gap at the Fermi level E_F, leading to 100% spin polarization at E_F, whereas the majority band behaves like a metal. The HMFs were discovered by theoretical band structure calculations for NiMnSb and PtMnSb [4]. Since then others have been found, such as CrO_2 [5, 6] the CMR-doped manganites [7, 8], the double perovskite Sr_2FeMoO_6 [2] and the diluted magnetic semiconductors (DMS) [9] like InMnAs; recently the zinc-blendes CrAs and CrSb were also proposed as HMFs [10, 11]. The current advantages in new materials are promising for engineering new spintronic devices in the near future. Thus, substantial attention is now being paid to finding new candidates for HMFs [12–14].

Unfortunately, CrO_2 and $La_{0.7}Sr_{0.3}MnO_3$ have only been verified to present practically 100% spin polarization at very low temperature and their spin polarizations decrease sharply with increasing temperatures; the Curie temperatures of DMSs are so low that DMSs have failed in the practical sense until now. The HM phases of the zinc-blende transition pnictides and chalcogenides are not their ground states, but the existing relatively high barriers between the ground states and the HM states result in the fact that the HM phases are very difficult to grow, or only very thin films can be obtained [12], which is not convenient in practice. On the other hand, the semi-Heusler alloys, such as NiMnSb, still remain attractive for technical spintronic applications due to their high Curie temperatures. Furthermore, it is worth noticing that the close structural similarity between the zinc-blende semiconductors and the semi-Heusler alloys makes the latter compatible with existing conventional semiconductor technology and thus very attractive for industrial applications. These facts motivated us to search for new HMFs in semi-Heusler alloys in NiCrM (M = P, As, Sb, S, Se and Te) by using first-principles band structure calculations within the density-functional theory (DFT). We predict that NiCrP, NiCrSe and NiCrTe are HMFs with HM gaps of 0.263, 0.047 and 0.102 eV, respectively, and other compounds are so-called nearly HMFs.

2. Computational details

First-principles electronic band structure calculations in the present work are based on the local spin density approximation (LSDA) for the exchange–correlation potential [15]. We use the method of full-potential linearized augmented plane waves (LAPWs) and local orbitals [15], where the potential and/or the charge density in the crystal are treated with no shape approximation. Relativistic effects are taken into account in the scalar style except for the spin–orbital coupling. The muffin-tin sphere radii R used are 2.2 au for Ni and Cr atoms, and 2.4 au for P, As, Sb, S, Se and Te atoms. Inside the atomic spheres the charge density and the potential are expanded in cubic harmonics up to $l = 6$. The radial basis functions of each LAPW are calculated up to $l = 8$ and the non-spherical potential contribution to the Hamilton matrix has an upper limit of $l = 4$. The Brillouin-zone integration is done with a modified tetrahedron method [16] and we use 60 $\boldsymbol{k}$ points in the first part of the irreducible Brillouin zone (IBZ). The density plane-wave cutoff is $RK_{\max} = 8.0$. The self-consistency is better than 0.001 me au^{-3} for charge density and spin density, and the stability is better than 0.01 mRyd for the total energy per cell.

3. Half-metallic ferromagnetism in NiCr M (M = P, As, Sb, S, Se, and Te)

3.1. Total energy and lattice parameter

We calculate the total energy for semi-Heusler alloys NiCrM (M = P, As, Sb, S, Se and Te) as a function of the lattice parameter, and perform both the paramagnetic and ferromagnetic configurations; in particular, E versus a curves for NiCrP and NiCrTe are shown as samples in figure 1. The predicted equilibrium lattice constants and the energy differences between the paramagnetic and ferromagnetic phases are given in table 1. It is clear that in all cases the ferromagnetic phases are more preferable in energy than the corresponding paramagnetic phases, i.e. the ferromagnetic phases of NiCrM (M = P, As, Sb, S, Se and Te) are about 0.83, 0.79, 0.82, 0.78, 1.02 and 0.96 eV more stable in energy than the corresponding paramagnetic phases, respectively. The predicted equilibrium lattice constants are 0.559, 0.568, 0.586, 0.552, 0.564 and 0.584 nm for ferromagnetic NiCrM (M = P, As, Sb, S, Se and Te), respectively.

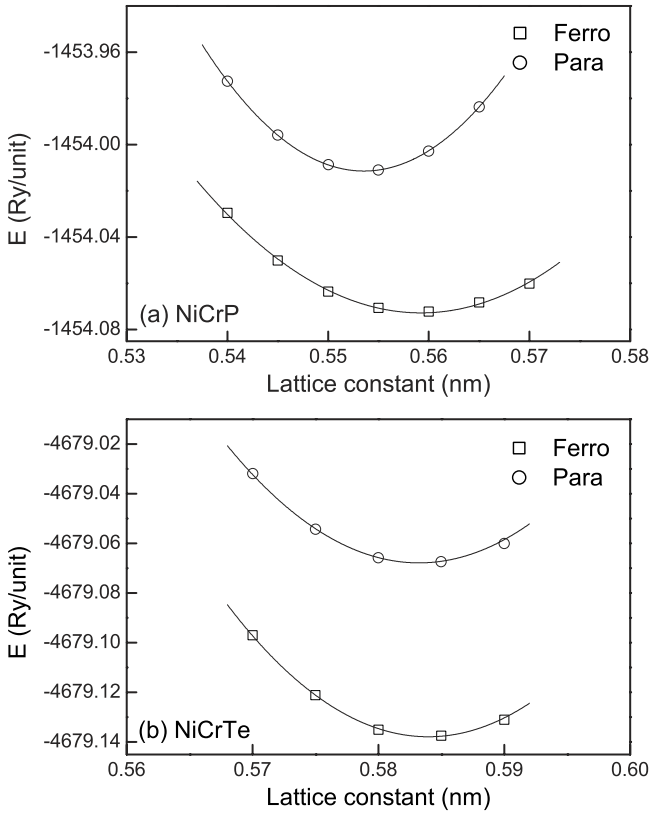

Figure 1. The total energy as a function of the lattice parameter for the paramagnetic and the ferromagnetic states of NiCrP and NiCrTe.

Table 1. The calculated equilibrium lattice parameter a of ferromagnetic phases and the energy difference ΔE between the paramagnetic states and the ferromagnetic states for NiCrM (M = P, As, Sb, S, Se and Te).

Compounds	NiCrP	NiCrAs	NiCrSb	NiCrS	NiCrSe	NiCrTe
a (nm)	0.559	0.568	0.586	0.552	0.564	0.584
ΔE (eV)	0.83	0.79	0.82	0.78	1.02	0.96

3.2. Half-metallic ferromagnetism in NiCrM (M = P, As, Sb, S, Se and Te)

The spin-dependent total and partial density of states (DOSs) for NiCrP at its theoretical equilibrium lattice parameter are shown in figure 2. As seen in this figure, the valence bands of NiCrP extend more than 7 eV below E_F. In the majority-spin component, Cr 3d states are mostly occupied and hybridized with Ni 3d electrons; however, in the minority-spin part, local and mostly non-hybridized Cr 3d states are found at about 1.35 eV above E_F. The P atoms provide s–p states to hybridize with d electrons and determine the degree of occupation of p–d orbitals. It should be noted that the partial low-lying part of s states of P atoms is very low in energy (about -11 eV) and not presented in figure 2. The spin moments of the Ni, Cr and P atoms are 0.115, 2.986 and -0.116 μ_B, respectively. Thus the total spin magnetic moment equals 2.985 μ_B/fu.

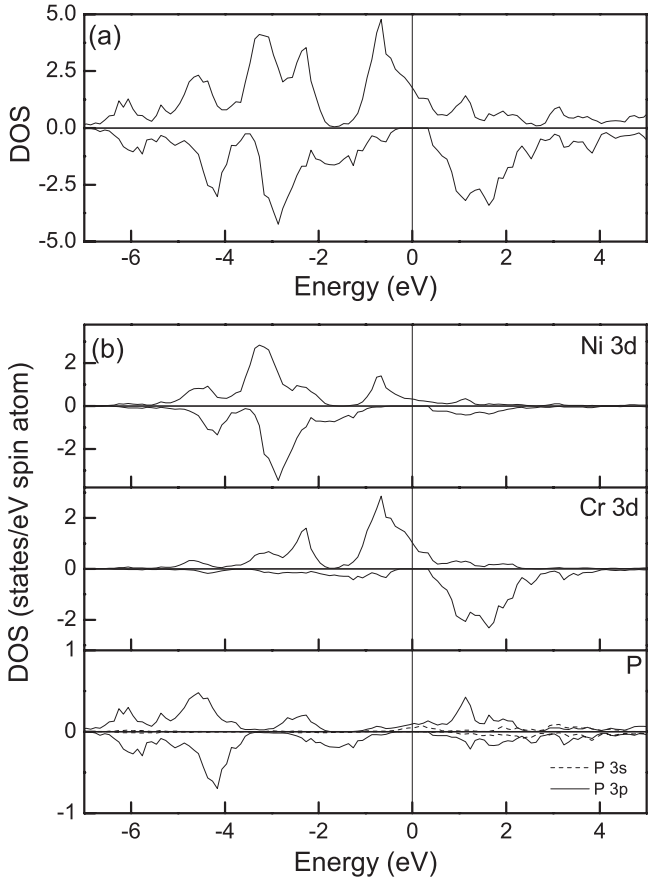

Figure 2. The spin-dependent total (upper panel) and partial (lower panel) DOSs of NiCrP at its predicted equilibrium lattice constant. There is a gap of around 0.696 eV around the Fermi level for the minority-spin bands.

We present the spin-dependent energy bands along high-symmetry directions in the Brillouin zone, as shown in figure 3. First, the P s electrons transform following the Γ_1 representation at the Γ point, being unaffected by the Ni and Cr exchange interaction; we do not show this band in figure 3 as the electrons are very low in energy and it is well separated by the other bands. The next triple-degenerate bands at around -3.8 eV are mainly due to the p electrons of the P atoms transforming following the Γ_{15} representation and have a strong admixture of Ni d states. The next double-degenerate Γ_{12} point at around -2.9 eV mainly originates from the Ni 3d electrons. Finally, due to the difference in the point-group symmetry of the semi-Heusler alloys from the full-Heusler alloys, the distinction between the t_{2g} d and p character of the electrons is lost and now the P atoms' p electrons can bind the t_{2g} d electrons [4, 17]. Through this mechanism in the minority bands the triple-degenerate bands (Γ_{15} at the Γ point) just below E_F are created by the bonding t_{2g} states of Ni and Cr with a small part of the P atoms' p states. Above the band gap the antibonding double-degenerate Cr e_g states (Γ_{12} at the Γ point) and the triple-degenerate t_{2g} states (Γ_{15} at the Γ point) can be found.

The majority-spin band structure is strongly metallic, while the minority-spin band structure shows a semiconducting gap around E_F. The calculated indirect Γ–X band gap for

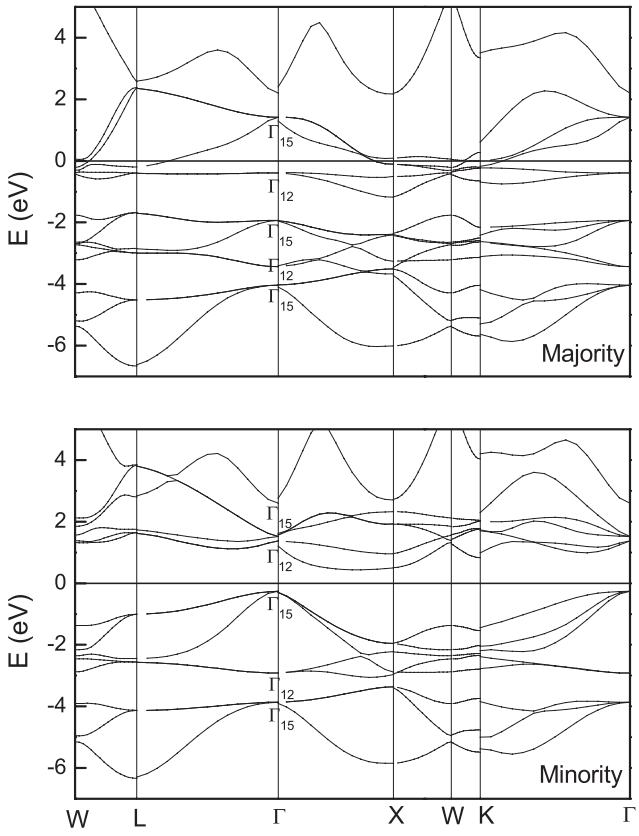

Figure 3. The band structure of NiCrP at the predicted equilibrium lattice constant. Note that the low-lying Γ_1 band arising from the s orbitals on P sites is very low in energy and not presented.

minority carriers is 0.696 eV around E_F for the minority-spin electrons of NiCrP. In addition, the Fermi level lies at 0.263 eV above the highest minority-spin valence bands. Hence, the 'spin-flip gap' (HM gap) has the value of 0.263 eV. It is worth noting that in our calculations the spin–orbit coupling is not taken into account, which can lift the band degeneracy and might destroy the indirect gap. But Youn and Min [18] reported that for NiMnSb the band structure with the spin–orbit coupling included was nearly the same as the semi-relativistic result, except that the change in the indirect gap was just about 0.06 eV and the magnitude of the spin–orbit splitting is only 0.02 eV for the triple-degenerate spin-down bands at Γ. Hence, the effect of the spin–orbit coupling cannot destroy the half-metallicity of NiCrP due to the sufficiently large indirect gaps.

Figure 4 shows the spin-dependent DOS of NiCrM (M = As, Sb, S, Se and Te). The spin-dependent bands for these compounds are also calculated, but the main characteristic is similar to that of NiCrP and not presented in this paper. The calculated band gaps, HM gaps and magnetic moments are given in table 2. As seen in figure 4, the Fermi levels of NiCrAs and NiCrSb are located at the highest valence bands and that of NiCrS is located just at the lowest conduction bands. Although the Fermi levels of these three compounds do not fall into the gap, they are very close to the edge of the gap. Thus, they are called nearly HMFs. For NiCrSe and NiCrTe, they are true HMFs with non-zero HM gaps of 0.047 and 0.102 eV, respectively.

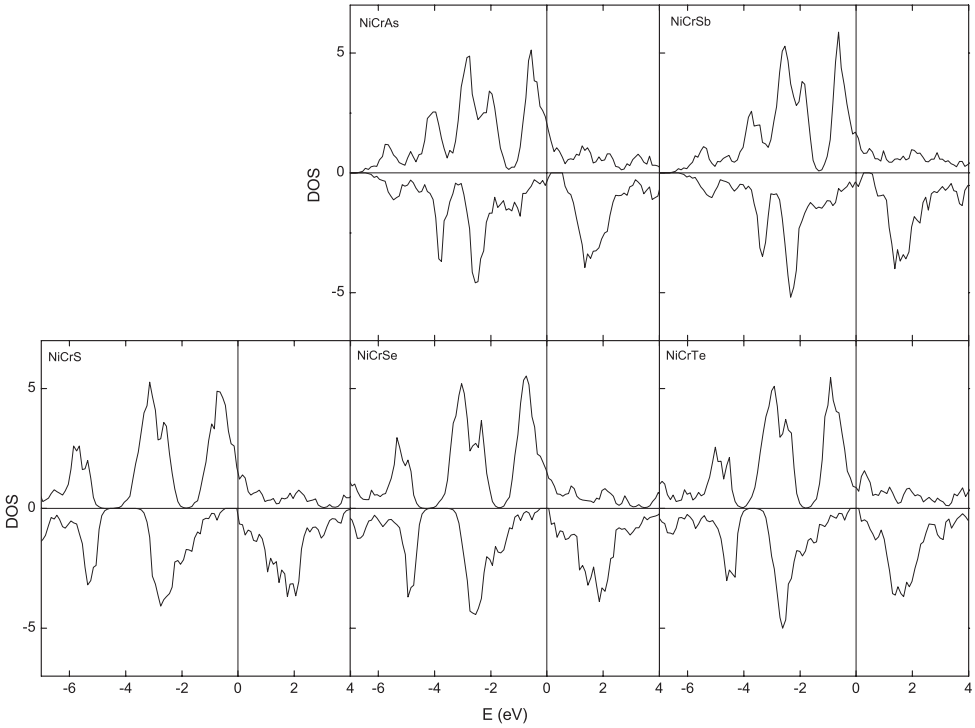

Figure 4. The spin-dependent total DOSs of NiCrM (M = As, Sb, S, Se and Te) at their predicted equilibrium lattice constants.

Table 2. Spin magnetic moments, band gaps and HM gaps at their predicted equilibrium lattice parameters for NiCrM (M = P, As, Sb, S, Se and Te).

m^{spin} (μ_{B})	Ni	Cr	M	Total	Band gap (eV)	HM gaps (eV)
NiCrP	0.115	2.986	−0.116	2.985	0.696	0.263
NiCrAs	0.085	2.989	−0.122	2.952	0.443	—
NiCrSb	0.047	2.994	−0.123	2.918	0.263	—
NiCrS	0.327	3.542	0.016	3.885	0.472	—
NiCrSe	0.297	3.703	−0.024	3.976	0.371	0.047
NiCrTe	0.243	3.769	−0.024	3.988	0.358	0.102

As seen in figures 2 and 4, the DOSs of these compounds are mainly characterized by the large exchange splitting of the Cr d states, which leads to the localized spin moment at the Cr site. The total magnetic moment in Bohr magnetons is simply the difference between the majority-spin and minority-spin occupied states. In HMFs, since the total number of the minority-spin states should be an integer due to the fact that all of them are occupied and the total charge number is an integer, the total magnetic moment should also be an integer. As given in table 2, we note that in our calculations Ni is ferromagnetically coupled to Cr with a small magnetic moment, while the sp atoms are all antiferromagnetically coupled to Cr except for NiCrS. Furthermore, the total magnetic moment per unit is close to an integer Bohr magneton, 3 μ_{B} for NiCrP and 4 μ_{B} for NiCrSe and NiCrTe, which are agreement with the HM behaviour shown in the DOS plots. The results are consistent with the Slater–Pauling rule, $M_{\text{t}} = Z_{\text{t}} - 18$, where Z_{t} denotes the total number of the valence electrons and M_{t} means

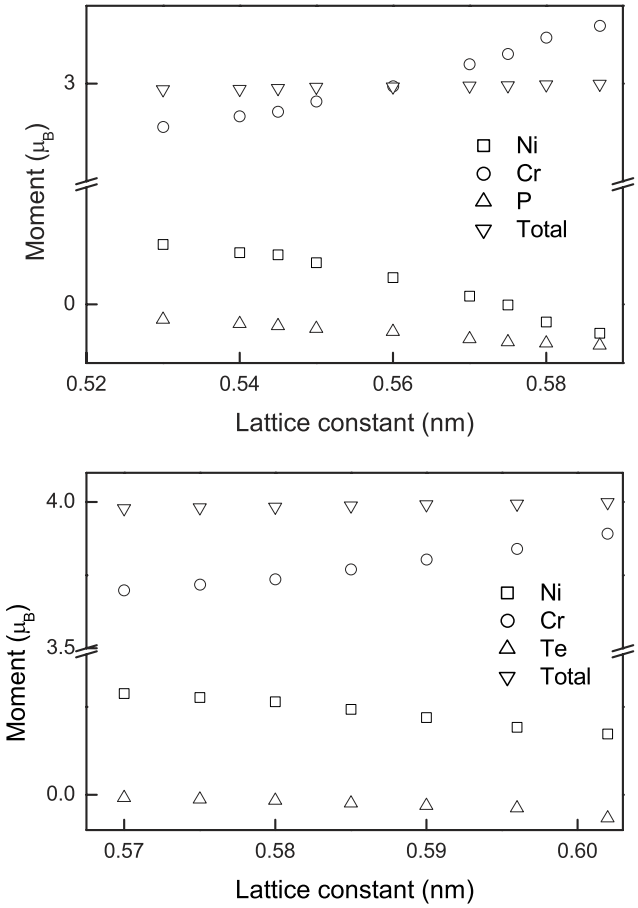

Figure 5. The lattice parameter dependence of the total magnetic moment, and the spin moments of Ni, Cr, P and Te atoms for NiCrP (upper panel) and NiCrTe (lower panel), respectively.

the total magnetic moment per unit cell, reported by Galanakis *et al* [17]. The spin moments of Ni for compounds containing the sp atom in the same column in the periodic table decrease with increasing atomic number, whilst the spin moments of Cr present the opposite behaviour. This implies that, for the compounds with the larger atomic number sp atoms, the hybridization between Ni and Cr is smaller than that of the compounds with the smaller atomic number sp atoms, which results in a smaller Ni spin moment and a larger Cr spin moment and eventually makes the Cr moment even more localized. The substitutions of sp atoms produce similar DOSs and are not responsible for the origin of the band gap since all compounds have gaps near the Fermi levels, but lead to a shift in the Fermi levels; thus the change of sp atoms can destroy the half-metallicity, such as in NiCrAs and NiCrSb.

4. Effect of the lattice parameter

For device applications, the materials will usually be grown as epitaxial films or heterostructures, the distortion of the lattice at the interface between the film and the substrate occurring frequently. Hence, the effects of the lattice parameter on the magnetic properties

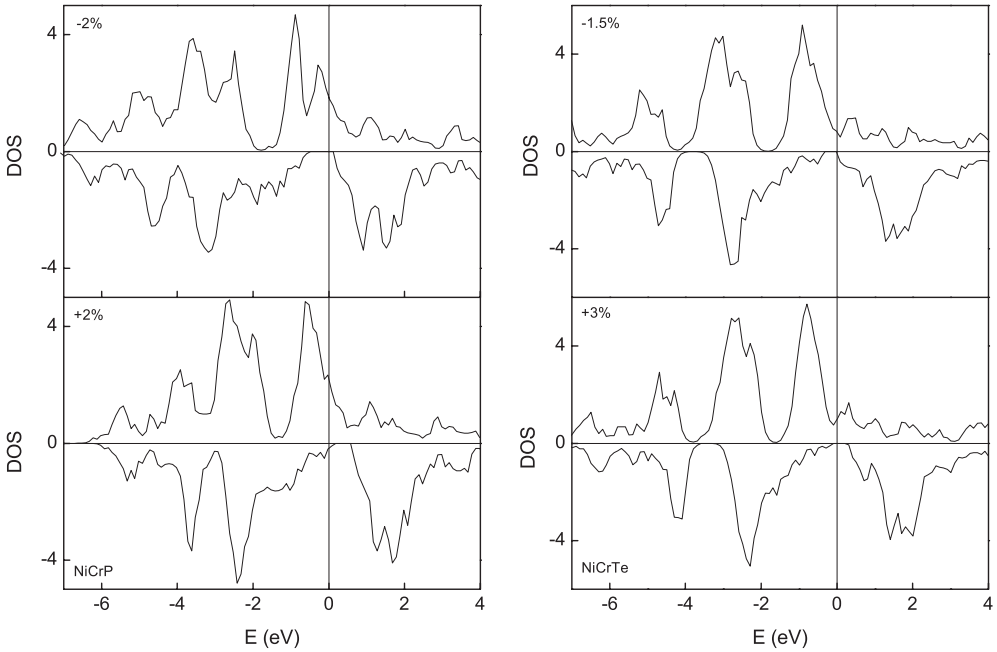

Figure 6. The total spin-dependent DOSs when the lattices of NiCrP and NiCrTe are expanded and contracted. The plus and minus signs refer to the expansion and contraction, respectively.

and the half-metallicity are crucial. In this section, our investigations mainly focus on the true HMFs, NiCrP and NiCrTe.

In figure 5, we present the lattice parameter dependence of the total magnetic moment and the spin moment of Ni, Cr, P and Te atoms. When we expand NiCrP and NiCrTe, the hybridization between Cr and Ni decreases, which leads to the fact that the Cr spin moment increases while the Ni spin moment decreases. The total magnetic moments per formula unit change little and remain at nearly 3 and 4 μ_B for NiCrP and NiCrTe, respectively. Especially, expansion and contraction change the total magnetic moment by less than 0.02 μ_B with respect to the predicted equilibrium lattice parameter, as in all cases the Fermi level falls inside the gap and the number of occupied minority-spin states changes little. Thus, any changes in the total moments are accompanied by changes of nearly equal magnitude and opposite sign in the number of occupied majority-spin and minority-spin states.

In figure 6 the DOSs are plotted for the contraction and expansion of NiCrP and NiCrTe with respect to the theoretically predicted values. Expansion moves E_F downwards in energy whereas contraction moves it upwards. The HM gap remains non-zero when we theoretically change the lattice parameter from -3% to less than +2% and from -1.5% to larger than +3% for NiCrP and NiCrTe, respectively. For NiCrSe, since the Fermi level is just below the right edge of the gap, any contraction will destroy the half-metallicity, but the expansion can make the HM behaviour more robust based on the above discussions and its half-metallicity can be preserved when the lattice is expanded by about +3.7% (the result is not presented in this paper). Here we should note that the equilibrium lattice constant predicted by the LDA calculation is underestimated by a few per cent (<3%) due to the so-called overbinding [19]. This effect makes the half-metallicity of the real material of NiCrP uncertain and a more accurate calculation including the correlation effects in a better formulation is needed to confirm

the HM behaviour. In contrast, the half-metallicity of NiCrSe and NiCrTe can be expected and confirmed in real materials since their half-metallicity can remain when the lattices are expanded by more than 3%.

5. Summary

We have investigated the electronic band structures and the magnetic properties of the semi-Heusler alloys NiCrM (M = P, As, Sb, S, Se and Te) to search for new candidate HMFs. We predict that NiCrP, and NiCrSe and NiCrTe, are likely HMFs with integer Bohr magnetons of total magnetic moments per formula unit of nearly 3 and 4 μ_B, respectively. This behaviour is attributed to the covalent hybridization between the d states of the Ni and Cr atoms, leading to the formation of bonding and antibonding bands with a gap in between. Other compounds are so-called nearly HMFs. When the lattice is expanded, the hybridization between Cr and Ni decreases, which leads to the fact that the Cr spin moment increases while the Ni spin moment decreases. The substitutions of sp atoms produce similar DOSs and are not responsible for the origin of the band gap, since all compounds have gaps near the Fermi levels, but lead to a shift in the Fermi levels; thus the change of sp atoms can destroy the half-metallicity.

Acknowledgments

We would like to acknowledge the financial support by the National Natural Science Foundation of China Grant Nos 50271083 and 50201020.

References

[1] Prinz G A 1995 *Phys. Today* **48** (April) 58
[2] Kobayashi K I, Kimura T, Sawada H, Terakura K and Tokura K 1998 *Nature* **395** 677
[3] Bandyopadhyay S 2000 *Phys. Rev.* B **61** 13813
[4] de Groot R A, Mueller F M, van Engen P G and Buschow K H J 1983 *Phys. Rev. Lett.* **50** 2024
[5] Kamper K P, Schmitt W, Guntherodt G, Gambino R J and Ruf R 1987 *Phys. Rev. Lett.* **59** 2788
[6] Brener N E, Tyler J M, Callaway J, Bagayoko D and Zhao G L 2000 *Phys. Rev.* B **61** 16582
[7] Soulen R J Jr, Byers J M, Osofsky M S, Nadgorny B, Ambrose T, Cheng S F, Broussard P R, Tanaka C T, Nowak J, Moodera J S, Berry A and Coey J M D 1998 *Science* **282** 85
[8] Park J H, Vescovo E, Kim H J, Kwon C, Ramesh R and Venkatesan T 1998 *Nature* **392** 794
[9] Akai H 1998 *Phys. Rev. Lett.* **81** 3002
[10] Galanakis I 2002 *Phys. Rev.* B **66** 012406
[11] Galanakis I and Mavropoulos P 2003 *Phys. Rev.* B **67** 104417
[12] Zhang M, Hu H, Liu G, Cui Y, Liu Z, Wang J, Wu G, Zhang X, Yan L, Liu H, Meng F, Qu J and Li Y 2003 *J. Phys.: Condens. Matter* **15** 5017
[13] Xie W H and Liu B G 2003 *J. Phys.: Condens. Matter* **15** 5085
[14] Xie W H, Xu Y Q and Liu B G 2003 *Phys. Rev. Lett.* **91** 037204
[15] Perdew J P and Wang W 1992 *Phys. Rev.* B **45** 13244
Blaha P, Schwarz K, Sorantin P and Tricky S B 1990 *Comput. Phys. Commun.* **59** 399
[16] Blöchl P, Jepson O and Andersen O K 1994 *Phys. Rev.* B **49** 16223
Blugel S, Akai H, Zeller R and Dederichs P H 1987 *Phys. Rev.* B **35** 3271
[17] Galanakis I, Dederichs P H and Papanikolaou N 2002 *Phys. Rev.* B **66** 134428
[18] Youn S J and Min B I 1995 *Phys. Rev.* B **51** 10436
[19] Asato M, Settels A, Hoshino T, Asada T, Blugel S, Zeller R and Dederichs P H 1999 *Phys. Rev.* B **60** 5202